

## GALVANOMAGNETIC INVESTIGATION OF THE METAL-NONMETAL TRANSITION IN SILICON\*

W. D. Straub, H. Roth, W. Bernard, and S. Goldstein

National Aeronautics and Space Administration/Electronics Research Center, Cambridge, Massachusetts

and

J. E. Mulhern, Jr.

University of New Hampshire, Durham, New Hampshire

(Received 26 June 1968)

High-field galvanomagnetic measurements are carried out on  $n$ - and  $p$ -type silicon in the concentration range corresponding to the metal-nonmetal transition. Abnormally large positive magnetoresistance is accompanied by a corresponding increase in the Hall coefficient with magnetic field. Expressions for resistivity and Hall coefficient are derived, and the predicted value of  $[\Delta\rho(H)/\rho(0)]/[\Delta R(H)/R(0)]$  is consistent with experimental results.

Currently there is considerable interest in the transition from nonmetallic to metallic conduction in a wide variety of materials.<sup>1</sup> A transition of this nature was first discussed by Mott,<sup>2</sup> who suggested that an insulator would undergo a sudden change to the metallic state at a lattice spacing corresponding to a critical overlap of atomic wave functions. It would appear that semiconductors are particularly well suited to investigations of such a transition since the impurity concentration and hence the impurity wave-function overlap can be varied in a controlled manner. However, the metal-nonmetal transition in semiconductors occurs continuously over a range of concentrations. In this Letter, we report on high-field galvanomagnetic studies of this gradual transition in silicon and their interpretation in terms of a band structure distorted by the random impurity potentials.

We have investigated the electrical transport properties of  $n$ - and  $p$ -type silicon doped with arsenic and boron, respectively, in the concentration range from  $5 \times 10^{18} \text{ cm}^{-3}$  to  $2 \times 10^{19} \text{ cm}^{-3}$ . This range corresponds to that investigated in phosphorus-doped silicon at lower magnetic fields by Tufte and Stelzer<sup>3</sup> and by Yamanouchi, Mizuguchi, and Sasaki.<sup>4</sup> All samples were oriented in the [100] direction, and experiments were carried out at temperatures down to 1.3°K and in magnetic fields up to 150 kOe.

Figure 1(a) shows the large longitudinal magnetoresistance  $\Delta\rho(H)/\rho(0)$  observed as a function of applied magnetic field for several  $n$ -type samples at 1.3°K. No normal longitudinal magnetoresistance would be expected for  $n$ -type silicon with current flow along the [100] axis. A small anisotropy of a few percent between the longitudinal and transverse magnetoresistance may be attributed to the normal component of the trans-

verse magnetoresistance. A corresponding relative change in the Hall coefficient  $\Delta R(H)/R(0)$  is shown in Fig. 1(b). Note that for a sample with a Hall voltage linear in the field  $R(H)/R(0) \equiv 0$  in the figure. (Although the data are not shown here, qualitatively similar results are obtained for the  $p$ -type material.) It is seen that both quantities decrease monotonically from hundreds of percent at the lower concentrations to only a few percent at the higher concentrations, and that the ratio

$$\frac{\Delta\rho(H)}{\rho(0)} / \frac{\Delta R(H)}{R(0)} \sim 2.$$

The results of resistivity and low-field Hall measurements as a function of temperature indicate that the sample having the lowest concentration still exhibits an impurity activation energy, whereas the sample having the highest concentration is approaching true degeneracy. In addition, the latter sample exhibits small Shubnikov-de Haas-type oscillations with a period characteristic of the conduction band. The transition from nonmetallic to metallic behavior can be considered to occur for As-doped silicon in the concentration range between these two limiting cases. It is interesting to observe that, in this transition range, the low-temperature mobility increases as the doping is increased, from  $\sim 20 \text{ cm}^2/\text{V sec}$  at  $n = 5.5 \times 10^{18} \text{ cm}^{-3}$  to  $\sim 130 \text{ cm}^2/\text{V sec}$  at  $n = 1.0 \times 10^{19} \text{ cm}^{-3}$ . The ratio of the low-temperature Hall concentration to the true concentration is always  $< 1$ , starting at  $\sim 0.5$  at  $n = 5.5 \times 10^{18} \text{ cm}^{-3}$  and asymptotically approaching unity in the limit of metallic conduction. The magnitude of the effects shown in Fig. 1 decreases rapidly as the temperature is raised above 1.3°K, becoming at 77°K only a few percent of its low-temperature value.

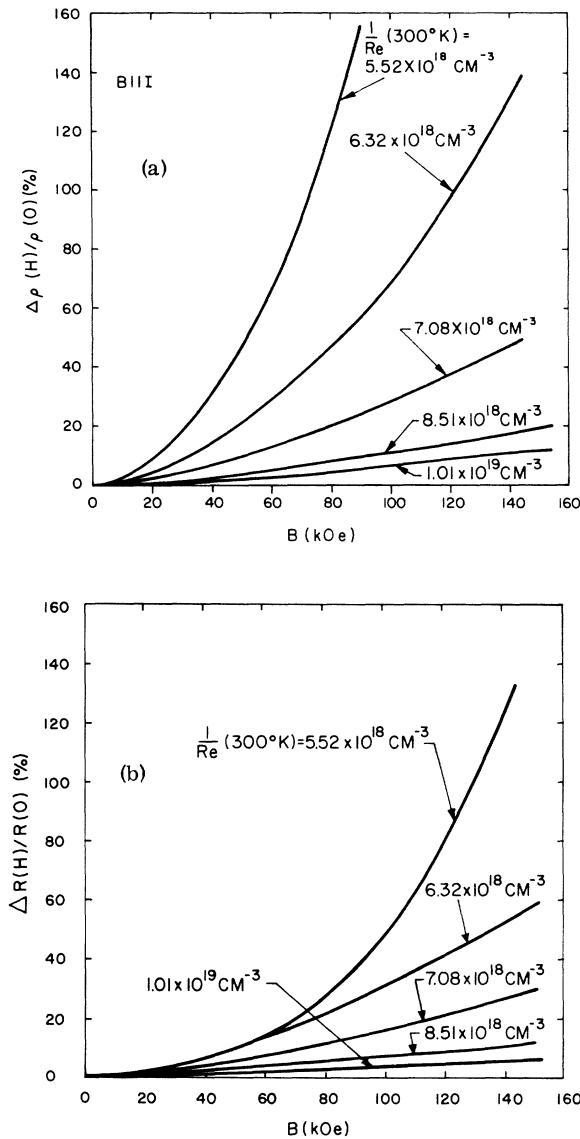


FIG. 1. (a) Magnetoresistance  $\Delta\rho(H)/\rho(0)$  and (b) relative change in the Hall coefficient  $\Delta R(H)/R(0)$  versus magnetic field for several arsenic-doped silicon samples at  $T = 1.3^\circ\text{K}$ .

The high-field anomalous behavior reported here, which occurs only in the transition range, should be contrasted with the low-field anomalous magnetoresistance in heavily doped semiconductors previously studied by a number of investigators.<sup>5-7</sup> The latter magnetoresistance is  $\sim 1\%$  or less, appears to saturate as the field is increased, and is negative in  $n$ -type and positive in  $p$ -type materials.<sup>8</sup>

The transport properties in the transition range are characterized neither by an impurity activation energy nor by a Fermi level lying in

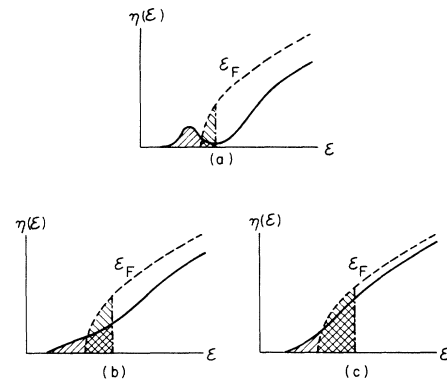


FIG. 2. Schematic density of states versus energy for a semiconductor in the metal-nonmetal transition range. Shown by the dashed curves for comparison is the intrinsic conduction band. (a) Lower end of range showing remainder of impurity band and energy gap; (b) middle of range showing distorted single conduction band; (c) upper end of range showing nearly metallic conduction.

the intrinsic conduction band. Rather it is necessary to consider a distorted band structure whose character is partly that of the random localized impurity states and partly that of the conduction-band states arising from the periodic host lattice. Figure 2 is a schematic representation of the modifications which must occur in the density of states  $\eta(\epsilon)$  as a function of energy as the impurity concentration is increased. Superimposed for comparison are dashed lines representing an unperturbed conduction band. The populated states at  $T = 0^\circ\text{K}$  are indicated for the distorted and unperturbed bands by the equal shaded areas. For the lowest concentrations, Fig. 2(a), the density of states corresponds to a distorted conduction band together with a slightly overlapping impurity band. An effective energy gap may still exist at these concentrations since  $\eta(\epsilon)$  is small at the Fermi level. Figure 2(b) shows a typical curve for an impurity concentration in the transition range. The distorted band structure arises from a significant admixture of both impurity-state and conduction-band wave functions. There is no longer evidence of an energy gap, but the density of states at the Fermi level is still appreciably less than the intrinsic conduction-band value. Figure 2(c) corresponds to the approach to the degenerate case in which the transport properties are characteristic of the undistorted conduction band. It is seen that the tail, arising from a partial localization of the low-energy states, remains, but that the density of states at the Fermi level is nearly

that of the intrinsic conduction band.

According to Mott, a metal-nonmetal transition should occur in a semiconductor when the impurity orbitals overlap sufficiently to preclude the formation of bound states. This critical concentration is given by<sup>2</sup>

$$n \sim (0.2/a^*)^3, \quad (1)$$

where  $a^* = \kappa\hbar/m^*e^2$  is the Bohr radius in a material of dielectric constant  $\kappa$  and effective mass  $m^*$ , and  $n$  is the impurity concentration. For hydrogenic impurities in silicon  $n \sim 4 \times 10^{18} \text{ cm}^{-3}$ , which is roughly the concentration associated with Fig. 2(a). However, according to the interpretation of Fig. 2, the transition from nonmetallic to metallic behavior begins at approximately this concentration but proceeds gradually as the concentration is further increased.

Alexander and Holcomb<sup>9</sup> have pointed out that the Mott transition in silicon can be deduced from Si<sup>29</sup> nuclear-spin relaxation experiments and from ESR experiments. They give the critical concentration as  $3 \times 10^{18} \text{ cm}^{-3}$  for phosphorus-doped material. Owing to the smaller Bohr orbits, this concentration should be somewhat higher in arsenic-doped silicon. In addition, Alexander and Holcomb on the basis of NMR measurements have deduced a second critical concentration  $\sim 2 \times 10^{19} \text{ cm}^{-3}$  for phosphorus-doped silicon characteristic of true metallic behavior. According to our interpretation, this corresponds to the completion of the transition, Fig. 2(c).

The influence of a magnetic field on a hydrogenic impurity state has been discussed theoretically by Yafet, Keyes, and Adams<sup>10</sup> and experimentally in germanium by Sadasiv.<sup>11</sup> The effect is characterized by a shrinking of the impurity wave functions and a corresponding increase in the activation energy. On this basis we assume that in the transition range the effect of a magnetic field is to enhance the localization of the wave functions, resulting in increased band distortion and a lower density of states at the Fermi level. Schematically this corresponds in Fig. 2 to the trend from (c) to (b) or from (b) to (a) with increasing magnetic field, with the exception that the concentration is held constant.

Since the distortion of the conduction band in the transition region is associated with the partial localization of the wave functions rather than with the inherent properties of the periodic host material, it is not appropriate to calculate the galvanomagnetic coefficients using a Boltzmann

equation and well defined Bloch states. Instead it is necessary to consider the localization of the wave functions and the scattering in a self-consistent way. In this spirit Edwards<sup>12,13</sup> has calculated the conductivity for a spherically symmetric band at  $T = 0^\circ\text{K}$  directly from the diagonal component of Kubo's general expression for the conductivity tensor<sup>14</sup>

$$\sigma_{lm} = \frac{e^2}{i\hbar m^*} \int_{-\infty}^0 dt \langle [x_l(t), p_m(0)] \rangle, \quad (2)$$

where  $x_l$  and  $p_m$  are the  $l$ th and  $m$ th components of the position and momentum operators, respectively, and  $\langle [ , ] \rangle$  denotes the equilibrium expectation value of the commutator. Edwards assumed that the localization of the wave functions gives rise to an uncertainty  $\Delta k$  in the wave vector, which is directly related to the scattering process. Averaging over the random spatial distribution of scattering potentials, neglecting the factor  $(1 - \cos\theta)$  in the momentum transfer cross section, and assuming that  $\Delta k \ll k$  at the Fermi level, he obtained a result which can be written in the form

$$\sigma = (ne^2\tau/m^*)g^2, \quad (3)$$

where the relaxation time  $\tau = \pi m^*/\hbar k_{\mathbf{F}} \Delta k$  and  $g = \eta(\epsilon_{\mathbf{F}})/\eta_0(\epsilon_{\mathbf{F}})$  is the ratio of the density of states of the distorted to that of the undistorted conduction band at the Fermi level.

The general expression for the Hall conductivity can be obtained from Eq. (2) as the linear term of the expansion of  $\sigma_{xy}$  in terms of a magnetic field  $H_z$  applied in the  $z$  direction, or, equivalently, from Kubo's general expression for the appropriate second-order current response function.<sup>14</sup> The explicit magnetic field dependence in this calculation arises from the  $\vec{p} \cdot \vec{A}$  term in the Hamiltonian. We have extended the Edwards technique to the evaluation of the Hall conductivity. Using the same approximations, we obtain at  $T = 0^\circ\text{K}$  the result

$$\sigma_H = (ne^3\tau^2/m^{*2})g^3. \quad (4)$$

The details of this calculation will be given in a forthcoming publication.

From Eqs. (3) and (4), the Hall coefficient is given by

$$R = \frac{\sigma_H}{\sigma^2} = 1/neg. \quad (5)$$

Since the experimentally determined low-temperature Hall concentration  $1/Re$  is always less than the true concentration  $n$ , Eq. (5) implies

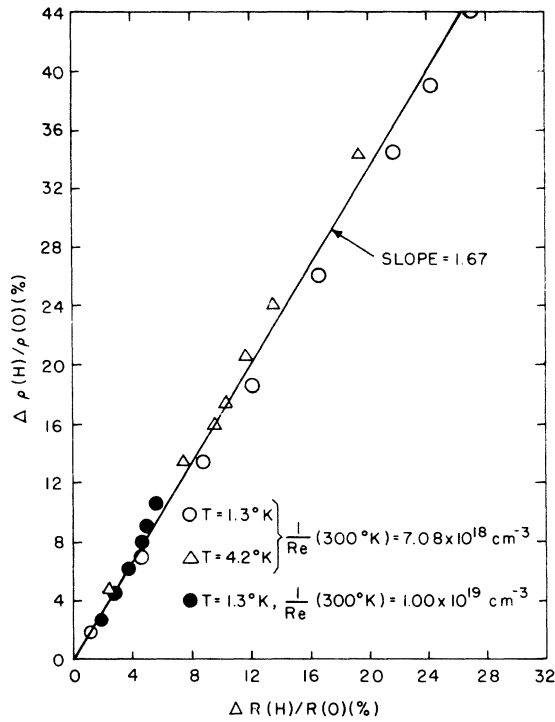


FIG. 3. Magnetoresistance  $\Delta\rho(H)/\rho(0)$  versus relative change in the Hall coefficient  $\Delta R(H)/R(0)$  for two arsenic-doped silicon samples in the transition range for various magnetic fields up to 150 kOe and two temperatures. The linear dependence with slope of 1.67 illustrates the consistency with theory.

that the value of the density-of-states ratio  $g$  is always  $<1$ .

In accordance with the discussion of Fig. 2, we assume that a magnetic field decreases the density of states at the Fermi level  $\eta(\epsilon_F)$  and hence decreases the quantity  $g$ . Letting  $g(H) = g(0) + \Delta g(H)$  and  $\tau(H) = \tau(0) + \Delta\tau(H)$  and retaining only the linear terms in  $\Delta g(H)$  and  $\Delta\tau(H)$ , we obtain from Eqs. (3) and (4)

$$\sigma(H) = \sigma(0) \left[ 1 + 2 \frac{\Delta g(H)}{g(0)} + \frac{\Delta\tau(H)}{\tau(0)} \right] \quad (6)$$

and

$$R(H) = \frac{\sigma_H(H)}{\sigma^2(H)} = R(0) \left[ 1 - \frac{\Delta g(H)}{g(0)} \right]. \quad (7)$$

Therefore the ratio of the magnetoresistance to the relative change in the Hall coefficient is given by

$$\frac{\Delta\rho(H)/\rho(0)}{\Delta R(H)/R(0)} = 2 + \frac{\Delta\tau(H)/\tau(0)}{\Delta g(H)/g(0)} \quad (8)$$

We note that since the magnetic field enhances

the localization of the wave functions around the impurities, thus decreasing the effective scattering cross section,  $\Delta\tau(H)$  should be  $>0$ . Recalling that  $\Delta g(H) < 0$ , we would therefore expect the numerical value of Eq. (8) to be  $<2$ .

In Fig. 3, we compare theory and experiment for two typical samples at  $T = 1.3$  and  $4.2^\circ\text{K}$  for fields up to 150 kOe. The ratio

$$\frac{\Delta\rho(H)/\rho(0)}{\Delta R(H)/R(0)}$$

can be characterized by a straight line having a slope of 1.67. Slopes for other samples have values falling between 1.5 and 1.9. These results are consistent with Eq. (8) and the assumption of decreasing  $g$  and increasing  $\tau$  with magnetic field.

While the data in Fig. 3 were obtained at finite temperatures, the present theory was derived assuming  $T = 0^\circ\text{K}$ . Although the magnitudes of  $\Delta R/R$  and  $\Delta\rho/\rho$  decrease by  $\sim 50\%$  as the temperature is raised from 1.3 to  $4.2^\circ\text{K}$ , the ratio of these quantities remains constant as shown in Fig. 3. This result is not surprising since, at low temperatures, one would expect that  $\Delta g$  and  $\Delta\tau$  in Eq. (8) would be replaced by suitable thermal averages, thus yielding small changes in the already small correction term

$$\frac{\Delta\tau/\tau(0)}{\Delta g/g(0)}$$

\*Part of this work was performed at Francis Bitter National Magnet Laboratory, which is supported at Massachusetts Institute of Technology by the Air Force Office of Scientific Research.

<sup>1</sup>First International Conference on the Metal-Nonmetal Transition, San Francisco, California, March, 1968 (to be published).

<sup>2</sup>N. F. Mott, *Phil. Mag.* **6**, 287 (1961).

<sup>3</sup>O. N. Tufte and E. L. Stelzer, *Phys. Rev.* **139**, A265 (1965).

<sup>4</sup>C. Yamanouchi, K. Mizuguchi, and W. Sasaki, *J. Phys. Soc. Japan* **22**, 859 (1967).

<sup>5</sup>W. Sasaki, C. Yamanouchi, and G. M. Hatoyama, in *Proceedings of the International Conference on Semiconductor Physics, Prague, 1960* (Academic Press, Inc., New York, 1961), p. 159.

<sup>6</sup>Y. Furukawa, *J. Phys. Soc. Japan* **17**, 630 (1962).

<sup>7</sup>H. Roth, W. D. Straub, W. Bernard, and J. E. Mulhern, Jr., *Phys. Rev. Letters* **11**, 328 (1963).

<sup>8</sup>H. Roth, W. D. Straub, W. Bernard, and J. E. Mulhern, Jr., *Bull. Am. Phys. Soc.* **12**, 404 (1967).

<sup>9</sup>M. N. Alexander and D. F. Holcomb, to be published.

<sup>10</sup>Y. Yafet, R. W. Keyes, and E. N. Adams, *J. Phys. Chem. Solids* **1**, 137 (1956).

<sup>11</sup>G. Sadasiv, Phys. Rev. **128**, 1131 (1962).<sup>12</sup>S. F. Edwards, Phil. Mag. **3**, 1020 (1958).<sup>13</sup>N. F. Mott, Advan. Phys. **16**, 49 (1967).<sup>14</sup>R. Kubo, J. Phys. Soc. Japan **12**, 570 (1957).

**EFFECTS OF ELECTRON-OPTICAL-PHONON INTERACTION  
IN THE COMBINED RESONANCE SPECTRA OF InSb**

B. D. McCombe and R. Kaplan

Naval Research Laboratory, Washington, D. C. 20390

(Received 24 June 1968)

The effects of electron-optical-phonon coupling on the combined resonance of both free and localized electrons have been studied in InSb. The results do not confirm the existence of a strong electron-TO-phonon interaction. Additional magneto-optical structure in the case of localized electrons appears to be due to discrete impurity excitations. The influence of conduction-band nonparabolicity on the impurity state binding energies has been observed.

Anomalies due to electron-optical-phonon coupling have recently been observed<sup>1</sup> in the combined resonance of electrons localized at impurities in InSb. The anomalies were interpreted as evidencing an electron-TO-phonon interaction comparable in strength to the electron-LO-phonon interaction which is responsible for the usual polaron effects. This result was somewhat surprising, since the analysis<sup>2-6</sup> of earlier observations of interband and electron cyclotron resonance absorption in InSb had excluded electron-TO-phonon coupling. Furthermore, there does not appear to be a satisfactory theoretical explanation for the coupling involving TO phonons.

The present Letter describes an experimental study of the effects of electron-optical-phonon coupling on the combined resonance of both free and localized electrons in InSb. Since the inclusion of the discrete "impurity" states of the localized electrons complicates the energy level structure, this structure is described initially in some detail. The methods used in obtaining and analyzing the data are then outlined. Results for the free-electron and localized-electron cases are presented separately, and are compared with those of earlier investigations.

The energy levels of interest in the present work are shown schematically in Fig. 1 for a magnetic field at which the cyclotron resonance energy is substantially larger than the impurity binding energy. For InSb, this situation obtains for fields greater than about 5 kG. The  $N=0$  and  $N=1$  free-carrier Landau levels are indicated by parabolas for effective spin vectors parallel ( $\uparrow$ ) and antiparallel ( $\downarrow$ ) to the magnetic field. Discrete impurity states of the electrons are identi-

fied by quantum-number sets  $(lm\lambda)$  in the manner of Wallis and Bowlden<sup>7</sup>; the Landau quantum number is given in terms of this set by  $N=l+\frac{1}{2}(m+|m|)$ . The solid arrows show the combined resonance transitions for free electrons ( $N=0; \uparrow$ )  $\rightarrow$  ( $N=1; \downarrow$ ), and localized electrons ( $000; \uparrow$ )  $\rightarrow$  ( $010; \downarrow$ ). Strong anomalies in combined resonance are expected for magnetic fields at which the optical phonon energy is comparable

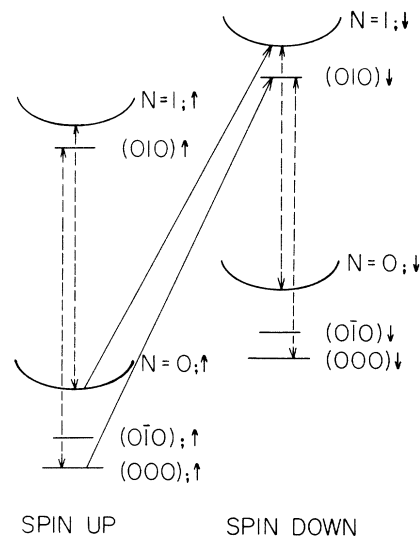


FIG. 1. Schematic representation of the energy levels of free and localized electrons in InSb in the high-field case. The lowest two Landau levels for both spin orientations are indicated by parabolas. Impurity states of importance in the present work have been included and are identified using the notation of Ref. 7. Combined resonance transitions are shown by solid arrows, while dashed arrows indicate spin-up and spin-down cyclotron resonance energies. The energy levels are not drawn to scale.